

Isotope effect on the superfluid density in conventional and high-temperature superconductors

Maksym Serbyn and Patrick A. Lee

Department of Physics, Massachusetts Institute of Technology, Cambridge, Massachusetts 02139, USA

(Received 23 September 2010; published 19 January 2011)

We investigate the isotope effect on the London penetration depth of a superconductor which measures n_S/m^* , the ratio of superfluid density to effective mass. We use a simplified model of electrons weakly coupled to a single phonon frequency ω_E , but assume that the energy gap Δ does not have any isotope effect. Nevertheless, we find an isotope effect for n_S/m^* which is significant if Δ is sufficiently large that it becomes comparable to ω_E , a regime of interest to high- T_c cuprate superconductors and possibly other families of unconventional superconductors with relatively high T_c . Our model is too simple to describe the cuprates and it gives the wrong sign of the isotope effect when compared with experiment, but it is a proof of principle that the isotope effect exists for n_S/m^* in materials where the pairing gap and T_c are not of phonon origin and have no isotope effect.

DOI: [10.1103/PhysRevB.83.024506](https://doi.org/10.1103/PhysRevB.83.024506)

PACS number(s): 74.25.Ha, 74.25.fc, 74.25.Kc

I. INTRODUCTION

While there is a general consensus that strong correlation governs the basic physics of high- T_c cuprates,¹ the role of electron-phonon interaction in determining T_c is still under debate. The isotope effect is often viewed as a useful tool which can provide information on this important issue. There is extensive isotope effect data on hole-doped cuprates and the following picture has emerged. There exists significant isotope effect on the transition temperature for underdoped cuprates, but none for overdoped ones. On the other hand, for all doping substantial isotope effect on the London penetration depth λ_{ab} has been observed.^{2,3} Recall that $\lambda_{ab}^{-2} \propto n_S/m^*$ is a direct measure of the ratio between the superfluid density n_S and the carrier mass m^* . The unusual isotope effect on T_c can be understood qualitatively by the following picture.¹ For underdoped samples the transition temperature is controlled by the phase stiffness⁴ $K_S = \hbar^2 n_S / 4m^*$. Hence, the isotope effect on T_c may be simply inherited from the isotope effect on n_S/m^* . On the other hand, in overdoped samples T_c is controlled by the pairing gap which has no isotope effect if phonons do not contribute significantly to its origin. Thus, the isotope effect of T_c can be qualitatively understood provided we accept the isotope effect on n_S/m^* . Then the puzzle is shifted to the origin of the isotope effect on n_S/m^* . Up to now there has been very little discussion in the literature on the isotope effect on n_S/m^* in superconductors. In this paper we address this important issue.

In Refs. 2 and 3 the authors suggested that the isotope effect on n_S/m^* is due to an isotope effect on the effective mass m^* . However, the effective mass is given by $m^*/m = 1 + \lambda$, where λ is the dimensionless electron-phonon coupling. Usually λ is not considered to have an isotope effect.⁵ This is because $\lambda = g^2 N(0) \omega_D$ and $g^2 \approx \langle I^2 \rangle / \omega_D$, where I is the coupling of the electron density to lattice deformation, which has no isotope dependence. This is supported by the direct experimental observation of Iwasawa *et al.*⁶ Using high-resolution laser angle-resolved photoemission spectroscopy (ARPES) measurements of electronic dispersion in $\text{Bi}_2\text{Sr}_2\text{CaCu}_2\text{O}_{8+\delta}$ (Bi2212), these authors study the influence of isotope oxygen substitution on the boson coupling “kink” in the electronic dispersion. The experiment clearly reveals an isotopic dependence of the kink energy, while it observes no change in the

effective electron mass. On the other hand, this experiment provides evidence for the coupling of phonon mode⁷ to electrons, which leads us to propose an alternative explanation for the isotope effect on n_S .

Our model disregards any effects of strong correlation and considers a clean superconductor with *s*- or *d*-wave singlet pairing. We suppose that there exists one phonon mode weakly coupled to the electron system. However, the superconducting order parameter is not related to the phonon mode, but rather induced by some other mechanism. Therefore, we ignore the isotope effect on the gap Δ and T_c , even though these effects can easily be added to lowest order in λ . We assume the standard adiabatic approximation for electron-phonon coupling⁸ and neglect Coulomb interaction. The only quantity which depends on the isotope mass is ω_E .

First, we present simple qualitative arguments that explain the existence of the isotope effect on n_S due to phonons using the sum rule which relates total spectral weight (SW) to the electron density and (bare) electron mass,

$$\frac{ne^2}{m} = \frac{2}{\pi} \int_0^\infty d\omega \sigma'(\omega), \quad (1)$$

where $\sigma'(\omega)$ is the dissipative part of the conductivity. The onset of superconductivity does not change the total SW, but redistributes it.⁹ Some part of the SW now goes to the δ -function response of the condensate, whose weight determines n_S/m^* , while the remaining goes to frequencies $\omega \geq 2\Delta$. This is visualized in Fig. 1. It displays the dissipative part of conductivity for normal metal, $\sigma'(\omega)$, that consists of a narrow Drude peak (since our sample is clean) along with a contribution from phonons at some characteristic frequency ω_E . Qualitatively, with the onset of superconductivity some SW from frequencies $\omega < \Delta$ goes to the δ peak and the SW from frequencies $\omega > \Delta$ goes to the optical conductivity of superconductor. Thus, if we have $\Delta \ll \omega_E$ (the case in weak coupling BCS theory), variation of ω_E would have no effect on SW that goes to the condensate response. This may be the reason why this problem has not received much attention in the literature up to now. If Δ and ω_E have the same order of magnitude, n_S/m^* responds to the change of ω_E and the isotope effect for n_S/m^* is present.

In the following sections we present calculations for the isotope effect for n_S/m^* based on the sum rule. In Sec. II we

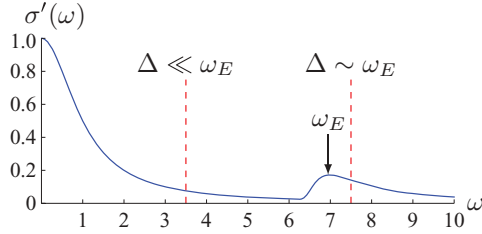


FIG. 1. (Color online) Qualitative form of the conductivity for a normal system. With the onset of superconductivity, all SW to the left of the corresponding vertical red dashed line goes to the condensate response.

introduce our toy model, then calculate conductivity and superfluid density. In Sec. III we discuss results and various approximations that were made. Finally, in the Appendix we present detailed calculations of the response kernel and conductivity.

II. CALCULATION FOR s - AND d -WAVE SUPERCONDUCTORS

In this section we present our calculation of the isotope effect on the superfluid density n_S . We note that both the experiment on the London penetration depth and the theory described in Eq. (1) give the combination n_S/m^* . From here on we simply define n_S as a product of n_S/m^* and m^* which is taken to be constant. We calculate the dissipative part of the conductivity due to phonons. After this, having the expression for the conductivity, via the sum rule, we get access to the superfluid density.

The theoretical model is a superconductor with electron-phonon interaction, described by the standard Fröhlich Hamiltonian. The superconducting order parameter (singlet pairing with s - or d -wave gap symmetry) is assumed to be *not related* to phonon mode under consideration. One may think about this pairing as induced by other phonon modes, strong correlation, or some different mechanism. The resulting Hamiltonian can be written as

$$H = H_{\text{BCS}} + H_{\text{ph}} + H_{\text{e-ph}}. \quad (2)$$

H_{BCS} is the BCS Hamiltonian, with the pairing in Cooper channel treated within mean-field theory (Coulomb interaction is neglected):

$$H_{\text{BCS}} = \sum_{\mathbf{p}} \xi_{\mathbf{p}} \Psi_{\mathbf{p}}^{\dagger} \tau_3 \Psi_{\mathbf{p}} - \frac{1}{2} \sum_{\mathbf{p}} \Psi_{\mathbf{p}}^{\dagger} (\Delta_{\mathbf{p}} \tau_+ + \Delta_{\mathbf{p}}^* \tau_-) \Psi_{\mathbf{p}}, \quad (3)$$

where $\xi_{\mathbf{p}}$ is the Bloch energy measured relative to the Fermi energy (we consider only one electron band that is coupled to one phonon mode) and τ_3 is the Pauli matrix. Electron field operators here are written as a vector in the Nambu space,

$$\Psi_{\mathbf{p}} = \begin{pmatrix} c_{\mathbf{p}\uparrow} \\ c_{\mathbf{p}\downarrow}^{\dagger} \end{pmatrix}, \quad (4)$$

with $c_{\mathbf{p},\uparrow}$, $c_{\mathbf{p},\uparrow}^{\dagger}$ being standard creation and annihilation operators for up (down) spin electrons. The Hamiltonian that describes the phonon mode and electron-phonon interaction is

written as

$$H_{\text{ph}} + H_{\text{e-ph}} = \sum_{\mathbf{k}} \omega(\mathbf{k}) b_{\mathbf{k}}^{\dagger} b_{\mathbf{k}} + \sum_{\mathbf{p}, \mathbf{p}'} g(\mathbf{p}, \mathbf{p}') (b_{\mathbf{p}'-\mathbf{p}} + b_{\mathbf{p}-\mathbf{p}'}^{\dagger}) \Psi_{\mathbf{p}}^{\dagger} \tau_3 \Psi_{\mathbf{p}}. \quad (5)$$

Here $\omega(\mathbf{k})$ is the (bare) phonon dispersion and $g(\mathbf{p}, \mathbf{p}')$ is the electron-phonon coupling. In what follows we use the Einstein approximation for the dispersion of phonons,

$$\omega(\mathbf{k}) = \text{const} = \omega_E, \quad (6)$$

and assume that our characteristic frequency ω_E is on order of the superconducting gap; that is, $\omega_E \sim \Delta$ (note that for BCS superconductivity $\omega_E \gg \Delta$). Moreover, we limit ourselves to leading-order corrections in the electron-phonon coupling that is assumed to be weak. Thus, we can neglect not only renormalization of the electron-phonon coupling (that is small in the parameter ω_E/E_F ¹⁰), but renormalization of the phonon dispersion as well.

A. Green's function and self-energy

Before we start our calculations of conductivity we need to consider the electron Green's function. Following standard procedure, we define the Green's function of electrons $G_{\mathbf{p}}(\tau)$ (which is a matrix in Nambu space) and phonons $D_{\mathbf{q}}(\tau)$ in imaginary time as

$$G_{\mathbf{p}}(\tau) = -\langle T_{\tau} [\Psi_{\mathbf{p}}(\tau) \Psi_{\mathbf{p}}^{\dagger}(0)] \rangle, \quad (7)$$

$$D_{\mathbf{q}}(\tau) = -\langle T_{\tau} [b_{\mathbf{q}}^{\dagger}(\tau) b_{\mathbf{q}}(0)] \rangle. \quad (8)$$

Fourier transform of bare Green's functions [which are denoted by index (0)] can be written in the form¹¹

$$[G_{\mathbf{q}}^0(i\omega_m)]^{-1} = i\omega_m - \xi_{\mathbf{q}} \tau_3 - \Delta \tau_1, \quad (9)$$

$$D_{\mathbf{q}}^0(i\omega_v) = \frac{1}{i\omega_v - \omega(\mathbf{q})} - \frac{1}{i\omega_v + \omega(\mathbf{q})}, \quad (10)$$

where $i\omega_m = (2n+1)\pi T$ and $i\omega_v = 2\nu\pi T$ are the Matsubara frequencies for fermions and bosons.

In order to find the Green's function of electrons in the presence of the electron-phonon interaction we note that the superconducting order parameter is not related to the phonon mode under consideration. Moreover, the electron-phonon coupling is small and we limit ourselves to the leading-order correction. Therefore, we can use perturbation theory to get access to the electron Green's function and there is no need to invoke the full Eliashberg strong coupling theory.^{12,13} Renormalization of the Green's function is given by the self-energy Σ_{ph} due to electron-phonon interaction:

$$[G_{\mathbf{p}}^R(\omega)]^{-1} = [G_{\mathbf{p}}^{0R}(\omega)] - \Sigma_{\text{ph}}^R(\mathbf{p}, \omega) = \tilde{\omega}^R(\omega) - \xi_{\mathbf{p}} \tau_3 - \tilde{\Delta}^R(\omega) \tau_1, \quad (11)$$

where $\tilde{\omega}(\omega)$ and $\tilde{\Delta}(\omega)$ are the renormalized ω and gap Δ , respectively.

It suffices to calculate the self-energy to the *leading order* in electron-phonon coupling. The expression for the self-energy in the Matsubara diagram technique can be read from the

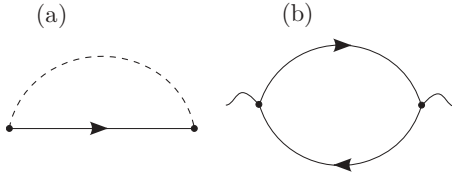


FIG. 2. Diagrams corresponding to the self-energy corrections (a) and conductivity (b).

diagram depicted in Fig. 2(a):

$$\Sigma_{\text{ph}}(\mathbf{p}, i\omega_n) = -T \sum_m \int (d\mathbf{p}') |g(\mathbf{p}, \mathbf{p}')|^2 \times D_{\mathbf{p}-\mathbf{p}'}^0(i\omega_n - i\omega_m) \tau_3 G_{\mathbf{p}'}^0(i\omega_m) \tau_3. \quad (12)$$

Here the Pauli matrix τ_3 (note that the self-energy is a matrix in the Nambu space) comes from the interaction vertex. Since we work to leading order of perturbation theory, we use the bare electron and phonon Green's functions. We proceed with analytical continuation (the detailed procedure is described in Refs. 13 and 14). Sums over positive and negative m are represented as contour integrals. Afterward, employing the spectral representation for the electron and phonon Green's functions (see Ref. 14), one has

$$\begin{aligned} \Sigma_{\text{ph}}^{R,A}(\mathbf{p}, \omega) &= - \int_{-\infty}^{\infty} (dx) \int_0^{\infty} d\Omega \alpha^2(\Omega) F(\Omega) \int d\xi_{\mathbf{p}'} \text{Im} [\tau_3 G_{\mathbf{p}'}^{0R}(x) \tau_3] \\ &\times \left[\frac{\tanh \frac{x}{2T} - \coth \frac{\Omega}{2T}}{x - \omega - \Omega \mp i\delta} - \frac{\tanh \frac{x}{2T} + \coth \frac{\Omega}{2T}}{x - \omega + \Omega \mp i\delta} \right], \quad (13) \end{aligned}$$

where $\alpha^2(\Omega)F(\Omega)$ is the spectral function of electron-phonon interaction (Eliashberg function) that consists of the product of effective electron-phonon coupling and phonon density of states. It is expressed through the electron-phonon interaction vertex as

$$\alpha^2(\Omega)F(\Omega) = \frac{\int_{\text{FS}} d^2 p \int_{\text{FS}} \frac{d^2 p'}{(2\pi)^3 v_F'} g(\mathbf{p}, \mathbf{p}') \delta(\Omega - \omega_{\mathbf{p}-\mathbf{p}'})}{\int_{\text{FS}} d^2 p}, \quad (14)$$

where v_F' is the Fermi velocity and integrations are over the Fermi surface (FS). Finally, we integrate over the loop momentum,¹⁵

$$\int d\xi_{\mathbf{p}'} \text{Im} [\tau_3 G_{\mathbf{p}'}^{0R}(x) \tau_3] = -i\pi \text{sgn} x \frac{x + \tau_1 \Delta}{\sqrt{x^2 - \Delta^2}}, \quad (15)$$

and put temperature $T = 0$. Expanding $\Sigma_{\text{ph}}^{R,A}(\mathbf{p}, \omega)$ in components we obtain for renormalized ω and Δ , which were defined earlier in Eq. (11),

$$\begin{aligned} \tilde{\omega}^{R,A}(\omega) &= \omega + \int_{-\infty}^{\infty} dx d\Omega \alpha^2 F(\Omega) \text{Re} \left[\frac{x \text{sgn} x}{\sqrt{x^2 - \Delta^2}} \right] \\ &\times \left[\frac{\theta(-x)}{x - \omega - \Omega \mp i\delta} + \frac{\theta(x)}{x - \omega + \Omega \mp i\delta} \right], \quad (16) \end{aligned}$$

$$\begin{aligned} \tilde{\Delta}^{R,A}(\omega) &= \Delta + \int_{-\infty}^{\infty} dx d\Omega \alpha^2 F(\Omega) \text{Re} \left[\frac{\Delta \text{sgn} x}{\sqrt{x^2 - \Delta^2}} \right] \\ &\times \left[\frac{\theta(-x)}{x - \omega - \Omega \mp i\delta} + \frac{\theta(x)}{x - \omega + \Omega \mp i\delta} \right]. \quad (17) \end{aligned}$$

It is convenient to introduce a dimensionless coupling constant λ defined to be responsible for the electron mass renormalization due to phonons:

$$m^* = m[1 + \lambda + O(\lambda)], \quad (18)$$

where m is bare and m^* is renormalized (measured in experiments, for example, in ARPES⁶) mass. The dimensionless coupling is expressed through the Eliashberg function (14) as

$$\lambda = 2 \int \frac{d\omega}{\omega} \alpha^2(\omega) F(\omega). \quad (19)$$

We work in the Einstein approximation, where the dispersion of the phonon mode does not depend on the momentum, $\omega_{\mathbf{p}} = \omega_E$. Using this, one can immediately infer from Eq. (14) that Eliashberg function $\alpha^2(\Omega)F(\Omega) \propto \delta(\Omega - \omega_E)$. The constant of proportionality can be read from Eq. (19), giving us the expression for the Eliashberg function that will be used in the remainder of this paper:

$$\alpha^2(\Omega)F(\Omega) = \frac{\omega_E \lambda}{2} \delta(\Omega - \omega_E). \quad (20)$$

In what follows we make use of the imaginary part of the renormalized frequency and gap, which can be easily inferred from Eqs. (16) and (17),

$$\tilde{\omega}^{R''}(\omega) = \pi \omega_E \lambda \frac{\theta(|\omega| - \omega_E - \Delta)(|\omega| - \omega_E)}{2\sqrt{(|\omega| - \omega_E)^2 - \Delta^2}}, \quad (21)$$

$$\tilde{\Delta}^{R''}(\omega) = \pi \omega_E \lambda \frac{\theta(|\omega| - \omega_E - \Delta) \Delta \text{sgn} \omega}{2\sqrt{(|\omega| - \omega_E)^2 - \Delta^2}}, \quad (22)$$

whereas for advanced functions we have

$$\tilde{\omega}^{A''}(\omega) = -\tilde{\omega}^{R''}(\omega), \quad \tilde{\Delta}^{A''}(\omega) = -\tilde{\Delta}^{R''}(\omega). \quad (23)$$

Not surprisingly, the imaginary part of the self-energy is present only for $\omega \geq \omega_E + \Delta$, that is, where the real excitation can be created. The square-root singularity that appears at this threshold would be smeared for a more realistic phonon spectrum.

B. Conductivity

Having the electron Green's functions at hand, we proceed to the calculations of the conductivity. Following the standard approach,¹¹ in order to calculate the conductivity we consider the response kernel $Q_{\alpha\beta}(\mathbf{k}, \omega)$ that relates current response to the vector potential:

$$j_{\alpha}(\mathbf{k}, \omega) = -\frac{ne^2}{m} Q_{\alpha\beta}(\mathbf{k}, \omega) A_{\beta}(\mathbf{k}, \omega). \quad (24)$$

The optical conductivity is expressed through Q as

$$\sigma_{\alpha\beta}(\mathbf{k}, \omega) = \frac{ne^2}{m} \frac{Q_{\alpha\beta}(\mathbf{k}, \omega)}{i\omega}. \quad (25)$$

The response kernel $Q_{\alpha\beta}(\mathbf{k}, \omega)$ can be calculated within the Kubo linear response method as a sum of the diamagnetic contribution and a current-current correlator¹¹:

$$\frac{ne^2}{m} Q_{\alpha\beta}(\mathbf{k}, \omega) = \frac{ne^2}{m} \delta_{\alpha\beta} - \mathcal{P}_{\alpha\beta}^R(\mathbf{k}, \omega), \quad (26)$$

where $\mathcal{P}_{\alpha\beta}^R(\mathbf{k}, \omega)$ is an analytic continuation to the real frequency of the (Fourier transformed) current-current correlator,

$$\mathcal{P}_{\alpha\beta}(\mathbf{r} - \mathbf{r}', \tau - \tau') = \langle T[\hat{j}_{1\alpha}(\mathbf{r}, \tau) \hat{j}_{1\beta}(\mathbf{r}', \tau')] \rangle. \quad (27)$$

The current operator $\hat{\mathbf{j}}_1(\mathbf{r})$ is defined as a paramagnetic part of the full current operator $\hat{\mathbf{j}}(\mathbf{r})$:

$$\begin{aligned}\hat{\mathbf{j}}(\mathbf{r}, \tau) &= \frac{ie}{2m} (\nabla_{\mathbf{r}'} - \nabla_{\mathbf{r}})_{\mathbf{r}' \rightarrow \mathbf{r}} c^+(\mathbf{r}') c(\mathbf{r}) - \frac{e^2}{m} \mathbf{A}(\mathbf{r}) c^+(\mathbf{r}) c(\mathbf{r}) \\ &\equiv \hat{\mathbf{j}}_1(\mathbf{r}, \tau) - \frac{e^2}{m} \mathbf{A}(\mathbf{r}) c^+(\mathbf{r}) c(\mathbf{r}).\end{aligned}\quad (28)$$

Since we consider the superconductor in the London limit, we can put $\mathbf{k} = 0$. Denoting $Q_{xx}(0, \omega) \equiv Q(\omega)$ we proceed to the calculation of $Q(\omega)$.

The current-current correlator $\mathcal{P}_{\alpha\beta}^R(k, \omega)$ is given by the sum of all possible diagrams with two external vertices corresponding to current operators. If we neglect vertex corrections (see discussion in Sec. III), in the leading order in the electron-phonon coupling we need to consider only the simplest diagram [Fig. 2(b)]. It is convenient to represent the diamagnetic contribution to $Q(\omega)$ through Green's functions of a normal metal.^{11,16} Combining the diamagnetic term with the current-current correlator given by the diagram in Fig. 2(b) we have

$$\begin{aligned}Q(i\omega_n) &= \frac{1}{2} \text{tr} \left\{ T \sum_{\omega_m} \int d\xi_{\mathbf{p}} [G_{\mathbf{p}}(i\omega_n + i\omega_m) G_{\mathbf{p}}(i\omega_m) \right. \\ &\quad \left. - G_{\mathbf{p}}^{\Delta=0}(i\omega_n + i\omega_m) G_{\mathbf{p}}^{\Delta=0}(i\omega_m)] \right\}.\end{aligned}\quad (29)$$

Starting from this expression we perform analytic continuation and integrate over the loop momentum. Analytical continuation is done in the standard way and is presented in detail in the literature^{14,16} and in the Appendix. After lengthy but straightforward calculations we get the following expression for the imaginary part of the response kernel $Q(\omega)$ at zero temperature:

$$\begin{aligned}Q''(\omega) &= \frac{1}{2} \text{Im} \int_{\Delta-\omega}^{-\Delta} dz \left[-\frac{g^{AA}(z+\omega, z) - 1}{\varepsilon^A(z+\omega) + \varepsilon^A(z)} \right. \\ &\quad \left. + \frac{g^{RA}(z+\omega, z) + 1}{\varepsilon^R(z+\omega) - \varepsilon^A(z)} \right].\end{aligned}\quad (30)$$

Where $\varepsilon^\alpha(\omega)$ with $\alpha = R, A$ is defined as

$$\varepsilon^\alpha(z) = \text{sgn } z \sqrt{[\tilde{\omega}^\alpha(z)]^2 - [\tilde{\Delta}^\alpha(z)]^2}, \quad (31)$$

and $g^{\alpha\beta}$ are the structure factors introduced in¹⁶

$$g^{\alpha\beta}(z_1, z_2) = \frac{\tilde{\omega}^\alpha(z_1) \tilde{\omega}^\beta(z_2) + \tilde{\Delta}^\alpha(z_1) \tilde{\Delta}^\beta(z_2)}{\varepsilon^\alpha(z_1) \varepsilon^\beta(z_2)}. \quad (32)$$

Using the expressions for the imaginary part of $\tilde{\omega}^{R,A}$ and $\tilde{\Delta}^{R,A}$ [Eqs. (21) and (22)], we expand to leading order in the corrections to the Green's function. After some calculations shown in the Appendix we arrive at the final answer, which can be expressed via complete elliptic integrals of the second kind, $E(x)$ and $K(x)$:

$$\sigma'(\omega) = \frac{ne^2 \pi \lambda \omega_E \omega_-}{m \omega^3} \left[E\left(\frac{\omega_-^2}{\omega_+^2}\right) - \frac{\Delta(\omega - \omega_E)}{\omega_+^2} K\left(\frac{\omega_-^2}{\omega_+^2}\right) \right], \quad (33)$$

where we used shorthand notation

$$\omega_\pm = \omega - \omega_E \pm 2\Delta. \quad (34)$$

In case when there is no superconductivity in our system, putting $\Delta = 0$ from (33) we reproduce the well-known result for the leading-order correction to the conductivity of normal metal due to phonons¹⁷:

$$\sigma'_{\text{N,e-ph}}(\omega) = \frac{ne^2}{m} \lambda \frac{\pi \omega_E (\omega - \omega_E)}{\omega^3} \theta(\omega - \omega_E). \quad (35)$$

$\sigma'(\omega)$ for the s -wave superconductor has been computed earlier by Allen.¹⁸ However the second term in Eq. (33) containing the elliptic function K is missing in Allen's formula. This difference is negligible when $\Delta \ll \omega_E$ but gives a small noticeable correction when $\Delta \gtrsim \omega_E$.

C. d -wave symmetry

The previous calculations can be easily generalized for the d -wave symmetry of pairing. We use the simplest possible model with the cylindrical Fermi surface with an axis parallel to the c axis of a crystal. The order parameter is supposed to have $d_{x^2-y^2}$ structure. It can be written as

$$\Delta(\mathbf{k}) = \Delta f \quad \text{with} \quad f = \cos 2\theta, \quad (36)$$

where θ is the angle between momentum (which lies in the a - b plane) and the a axis.

First we recalculate our corrections to the electron Green's function. In contrary to the s -wave case, the gap $\Delta(\mathbf{k})$ depends on the direction of momentum. Therefore, the previous answer for the s -wave case needs to be averaged over the Fermi surface. Averaging is defined as

$$\langle X \rangle_{\text{FS}} = \int_0^{2\pi} (d\theta) X(|\cos 2\theta|). \quad (37)$$

Gap renormalization $\tilde{\Delta}^R(\omega) - \Delta = 0$ vanishes under averaging over angle, while the imaginary part of the renormalization of ω reads

$$\begin{aligned}\tilde{\omega}^{R''}(\omega) &= \frac{\pi \omega_E \lambda}{2} \theta(|\omega| - \omega_E) \left\langle \frac{|\omega| - \omega_E}{\sqrt{(|\omega| - \omega_E)^2 - \Delta^2 f^2}} \right\rangle_{\text{FS}} \\ &= \frac{\pi \omega_E \lambda}{2} \theta(|\omega| - \omega_E) \kappa \left(\frac{|\omega| - \omega_E}{\Delta} \right),\end{aligned}\quad (38)$$

where $\kappa(x)$ is defined as

$$\kappa(x) = \frac{2}{\pi} \begin{cases} x K(x^2) & \text{for } x \leq 1, \\ K(x^{-2}) & \text{for } x > 1. \end{cases} \quad (39)$$

We repeat calculations of conductivity with $\tilde{\Delta}(\omega) = \Delta$ and the new expression for $\tilde{\omega}^{R''}(\omega)$. Correction to the conductivity to leading order in the electron-phonon coupling is

$$\sigma'(\omega) = \frac{ne^2}{m} \frac{2}{\omega^3} \left\langle \int_{\Delta|f|-\omega}^{-\Delta|f|} dz \frac{z \tilde{\omega}^{R''}(z+\omega)}{\sqrt{z^2 - \Delta^2}} \right\rangle_{\text{FS}}. \quad (40)$$

Interchanging averaging over FS and integration over frequency we have two different expressions for $\omega_E \geq \Delta$ and $\omega_E < \Delta$. When $\omega_E \geq \Delta$ we obtain

$$\begin{aligned}\sigma'(\omega) &= \frac{ne^2}{m} \frac{\pi \omega_E \lambda}{\omega^3} \theta(\omega - \omega_E) \\ &\quad \times \int_{\omega_E - \omega}^0 dz \kappa \left(\frac{|z + \omega| - \omega_E}{\Delta} \right) \kappa \left(\frac{|z|}{\Delta} \right),\end{aligned}\quad (41)$$

while for $\omega_E < \Delta$ we have a more complicated expression involving the elliptic integral of the first kind $F(\sin \phi; k)$:

$$\sigma'(\omega) = \frac{ne^2}{m} \frac{\pi \omega_E \lambda}{\omega^3} \theta(\omega - \omega_E) \left[\int_{\Delta - \omega}^0 dz \kappa \left(\frac{|z + \omega| - \omega_E}{\Delta} \right) \kappa \left(\frac{|z|}{\Delta} \right) + \frac{2}{\pi} \int_{\omega_E - \omega}^{\Delta - \omega} dz \kappa \left(\frac{|z + \omega| - \omega_E}{\Delta} \right) F \left(\frac{z + \omega}{\Delta}; \frac{\Delta^2}{z^2} \right) \right]. \quad (42)$$

Figure 3 illustrates calculated correction to the conductivity for the normal metal and superconductor with s - or d -wave pairing for $\omega_E = 1.5\Delta$ as a function of ω/Δ .

D. Isotope effect for superfluid density n_S

Using our explicit results for the conductivity, by means of the sum rule, we get access to the superfluid density. Initially, the sum rule is formulated as

$$\frac{ne^2}{m} = \frac{2}{\pi} \int_0^\infty d\omega \sigma'(\omega), \quad (43)$$

where n and m are mass and concentration of electrons, respectively, while $\sigma'(\omega)$ is the dissipative part of the conductivity.

Let us first apply the sum rule to our system when there is no superconductivity, that is, $\Delta = 0$. We assume that the mean free path is big, thus scattering time due to impurities τ satisfies $\tau \omega_E \gg 1$. Then, in addition to the very narrow Drude peak at $\omega = 0$, $\sigma_D(\omega)$, we have the small correction due to phonons, $\sigma'_{N,e-ph}(\omega)$, that starts at ω_E [see Eq. (35)]. The calculation of the SW of the Drude peak from the sum rule goes as follows:

$$\begin{aligned} \frac{2}{\pi} \int_0^\infty d\omega \sigma'_D(\omega) &= \frac{ne^2}{m} - \frac{2}{\pi} \int_0^\infty d\omega \sigma'_{N,e-ph}(\omega) \\ &= \frac{ne^2}{m} - \lambda \frac{ne^2}{m} = \frac{ne^2}{m^*} [1 + O(\lambda^2)], \end{aligned} \quad (44)$$

where $m^* = m(1 + \lambda)$ [see Eq. (18)]. We see that the SW of $\sigma'_{N,e-ph}(\omega)$ does not depend on ω_E and the sum rule reproduces the correct answer for the SW of the Drude peak with the renormalized mass.

With the onset of the superconductivity the picture does not change drastically. The dissipative part of the conductivity consists of the δ function with the weight given by $n_S e^2 / m^*$

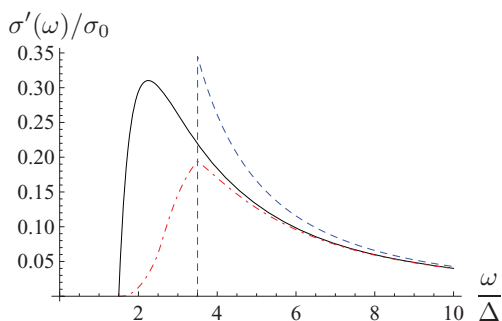


FIG. 3. (Color online) Correction to the dissipative part of conductivity $\sigma'(\omega)$ due to phonons for normal metal (solid black line) and superconductor with s or d wave symmetry (dashed blue and dash-dotted red curves, correspondingly) for $\omega_E = 1.5\Delta$. σ normalized to $\sigma_0 = \frac{ne^2}{m} \lambda$; Drude peak and δ -function response of condensate are not shown.

(response of the condensate) and the small contribution due to electron-phonon interaction $\sigma'(\omega)$ [calculated in Eq. (33) and Eqs. (41) and (42) for s and d -wave pairing]. The sum rule implies for n_S :

$$n_S = n - \frac{2m}{\pi e^2} \int_{2\Delta}^\infty d\omega \sigma'(\omega). \quad (45)$$

From Eqs. (33) and (41), the superfluid density n_S can be easily computed. It depends on ω_E , thus giving nonzero isotope effect on superconducting density. Results of the numerical computations of $(n_S - n)/\lambda$ as a function of ω_E/Δ are shown in Fig. 4.

Based on the dependence of n_S on ω_E , an isotope coefficient β can be easily calculated. It is defined as²

$$\beta = -\frac{d \log \lambda_{ab}^{-2}}{d \log M_O} = \frac{1}{2} \frac{d \log \lambda_{ab}^{-2}}{d \log \omega_E}, \quad (46)$$

where the usual relation between the phonon characteristic frequency and the atomic mass M_O (in experiment this is usually the atomic mass of oxygen) was assumed:

$$\frac{\Delta \omega_E}{\omega_E} = -\frac{1}{2} \frac{\Delta M_O}{M_O}. \quad (47)$$

Results for β are shown in the Fig. 5. Notably, for both s - and d -wave symmetry, the isotope coefficient has maximum modulus when $\omega_E \sim \Delta$, while when $\omega_E \gg \Delta$, β vanishes in either case. Such behavior naturally follows from our qualitative arguments, presented in the Introduction. However, note that β approaches zero from positive and negative values for the s -wave and d -wave pairing, respectively.

III. DISCUSSION

Although our toy model proves that isotope effect on the superfluid density can exist due to phonons, it gives an effect of the opposite sign to the experimentally measured. For example, in Ref. 2, for YPrBaCuO, $\beta = 0.38$ for $x = 0.3$ and $\beta = 0.71$

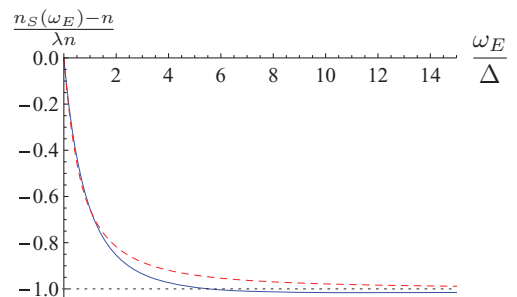


FIG. 4. (Color online) Correction to superfluid density for superconductor with s -wave (solid blue) or d -wave (dashed red) symmetry.

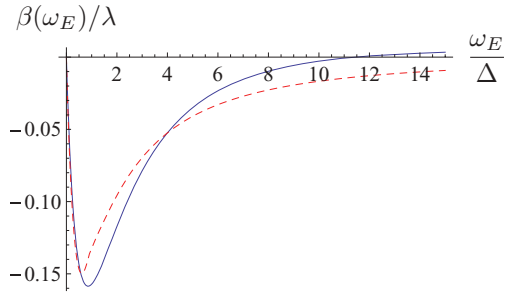


FIG. 5. (Color online) Isotope coefficient β as a function of ω_E in our model for superconductor with s -wave (solid blue) or d -wave (dashed red) symmetry.

for $x = 0.4$, while our model predicts the isotope coefficient of order of $\beta \sim -0.1$ for $\lambda \sim 1$.

The opposite sign of isotope coefficient leads us to a discussion of the limitations of our model. We treated the electron-phonon interaction as being weak, which is not really the case. As can be inferred from the experiment,^{6,7} the coupling constant is of order one. However, the qualitative features of our result should not change. The second approximation was the neglect of vertex corrections. The justification of this has been given in Ref. 18. Since for normal metal ladder diagrams give minor effects, we expect this to be the case for superconductors as well.

The most serious limitation of our model with respect to high- T_c superconductors is the neglect of strong correlation effects. The minimum requirement would be to reproduce the fact that n_S is proportional to the doping-hole concentration x due to the proximity to the Mott transition and not to the electron density $1 - x$ as in our toy model. Furthermore, from the point of view of the sum-rule argument, it is known that strong correlation gives rise to an incoherent background at finite frequencies, the so-called mid-infrared peak, even before phonons are taken into account. This incoherent background is missing in our toy model. What is needed is clearly a model which includes both Coulomb repulsion and coupling to phonons, such as the Hubbard-Holstein model. There has been considerable progress in this difficult problem, as given in a recent review.¹⁹ However, up to now these considerations involve polaron physics and phonons as a pairing mechanism and cannot be directly compared to our model. We note that very recently there has been an attempt to include correlations and strong coupled phonon effect together.²⁰ Even though our result does not agree with the experiment, the important message of the present paper is a proof of principle that isotope effect in n_S/m^* is possible even if the pairing is not due to phonons.

Finally, the isotope effect on the superfluid density discussed in this paper should be applicable to conventional superconductors in the clean limit with minor extensions. To linear order in λ , it is straightforward to include coupling to a distribution of phonon modes. Furthermore, we can easily include the isotope effect on the energy gap Δ in our consideration. In weak coupling BCS theory, Δ is proportional to ω_E and the ratio Δ/ω_E has no isotope dependence. Then our theory trivially predicts no isotope effect on n_S/m^* . Including $\mu^* = \mu/\log(\epsilon_F/\omega_E)$ in the T_c formula will introduce some

isotope dependence in Δ/ω_E . However, in most superconductors $\omega_E/\Delta \gg 1$ and from Fig. 5 we see that the predicted effect is very small. Recently s -wave superconductors with relatively large T_c and energy gap have been discovered. Examples are MgB_2 ²¹ and doped fullerenes. While coupling to certain high-frequency phonons may be responsible for the pairing, there exist in these materials lower-frequency phonons with frequency ω_0 which may bring us to the regime of intermediate ω_0/Δ . It will be interesting to search for the isotope effect on the penetration depth in these materials (provided they are in the clean limit). In addition, the new class of Fe-based superconductors have a rather large ratio of Δ/ω_E and should exhibit the isotope effect on the penetration depth according to our theory.

APPENDIX: DERIVATION OF THE RESPONSE KERNEL AND CONDUCTIVITY

In this Appendix, following Refs. 11 and 16 we derive the response kernel $Q(\omega)$ and dissipative part of the optical conductivity $\sigma'(\omega)$ due to the electron-phonon interaction. Starting from the expression for $Q(i\omega_n)$ [Eq. (29)], we do analytic continuation to the real frequencies. Performing integration over ξ_p and setting temperature to zero, we arrive at the final expression for the response kernel. Afterward, using corrections to the self-energy and expanding in the electron-phonon coupling, we get the conductivity.

The Matsubara sum in (29) is represented as a contour integral in the standard way,

$$\begin{aligned} & \sum_m G_p(\omega_n + \omega_m) G_p(\omega_m) \\ &= \frac{1}{4\pi i} \int_{C_0} dz \tanh \frac{z}{2T} G_p(\omega_n - iz) G_p(-iz), \end{aligned} \quad (\text{A1})$$

where the contour C_0 surrounds poles of $\tanh \frac{z}{2T}$ that lie on the imaginary axis (see Fig. 6). Having in mind subsequent integration over ξ_p , it is convenient to represent the electron Green's function (11) as¹⁶

$$\begin{aligned} G_p(i\omega_n) = & \frac{1}{2\varepsilon(i\omega_n)} \left[\frac{\tilde{\omega}(i\omega_n) + \tau_3\varepsilon(i\omega_n) + \tau_1\tilde{\Delta}(i\omega_n)}{\varepsilon(i\omega_n) - \xi_p} \right. \\ & \left. + \frac{\tilde{\omega}(i\omega_n) - \tau_3\varepsilon(i\omega_n) + \tau_1\tilde{\Delta}(i\omega_n)}{\varepsilon(i\omega_n) + \xi_p} \right], \end{aligned} \quad (\text{A2})$$

where $\varepsilon(\omega)$ is defined as

$$\varepsilon(\omega) = \sqrt{\tilde{\omega}^2(\omega) - \tilde{\Delta}^2(\omega)}. \quad (\text{A3})$$

Originally, $G_p(i\omega_n)$ in Eq. (A2) is defined only at the discrete set of Matsubara frequencies on the imaginary axis. Analytic properties of $G_p(z)$ in the complex plane are related to the properties of function $\varepsilon(z)$. We suppose that on the imaginary axis $\varepsilon(z)$ is a well-defined function. Let us denote a point where $\varepsilon(z)$ has an essential singularity as ω_Δ . We argue that ω_Δ is real. Indeed, on the real axis the self-energy correction has a nonzero imaginary part only for frequencies above the threshold, $\omega \geq \Delta + \omega_E$. Therefore, ω_Δ is real and $\omega_\Delta = \Delta + O(\lambda)$, where $O(\lambda)$ are corrections of order of λ . Drawing branch cuts from points $\pm\omega_\Delta$ to infinity (they are shown in red zigzags in Fig. 6),

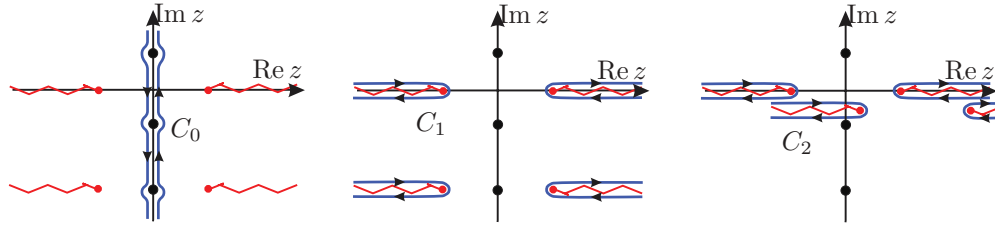


FIG. 6. (Color online) Deformation of integration contour during analytical continuation. Branch cuts of Green's functions are shown by red zigzags and starts at ω_Δ and $\omega_\Delta - i\omega_m$. When we do analytical continuation from $\omega_n \rightarrow -i\omega$, all four branch cuts lie on the real axis.

we make $\varepsilon(z)$ a well-defined function in the whole complex plane.

Retarded and advanced Green's functions $G_p^{R,A}(z)$ are given by the value of $G_p(i\omega_n)$ at the upper (lower) side of the branch cut. They are obtained from Eq. (A2) by replacing functions $\tilde{\omega}(z)$, $\tilde{\Delta}(z)$, and $\varepsilon(z)$ with their analytic continuation to the upper (lower) side of cuts. These are denoted as $\tilde{\omega}^{R,A}(z)$, $\tilde{\Delta}^{R,A}(z)$, and $\varepsilon^{R,A}(z)$, correspondingly, where first

two functions were calculated in the Sec. II A, and last function is defined as

$$\varepsilon^\alpha(z) = \text{sgn } z \sqrt{[\tilde{\omega}^\alpha(z)]^2 - [\tilde{\Delta}^\alpha(z)]^2}, \quad (\text{A4})$$

where $\alpha = R, A$. Now we deform the contour from C_0 to C_1 (see Fig. 6) and analytically continue to the real external frequency $\omega_n \rightarrow -i\omega$. As a result, the Matsubara sum (A1) is written as

$$\begin{aligned} \sum_m G_p(\omega_n + \omega_m) G_p(\omega_m) &= \frac{1}{4\pi i} \int_{\omega_\Delta}^{\infty} dz \tanh \frac{z}{2T} \{ [G_p^R(z) - G_p^A(z)] [G_p^R(z + \omega) + G_p^A(z - \omega)] \\ &\quad + [G_p^R(-z) - G_p^A(-z)] [G_p^R(-z + \omega) + G_p^A(-z - \omega)] \}. \end{aligned} \quad (\text{A5})$$

The trace of the product of two Green's functions $G^\alpha(z_1)G^\beta(z_2)$ with $\alpha, \beta = R, A$ can be written as

$$\begin{aligned} 2 \text{tr } G^\alpha(z_1) G^\beta(z_2) &= \frac{g^{\alpha\beta}(z_1, z_2) + 1}{[\varepsilon^\alpha(z_1) - \xi_p][\varepsilon^\beta(z_2) - \xi_p]} + \frac{g^{\alpha\beta}(z_1, z_2) + 1}{[\varepsilon^\alpha(z_1) + \xi_p][\varepsilon^\beta(z_2) + \xi_p]} + \frac{g^{\alpha\beta}(z_1, z_2) - 1}{[\varepsilon^\alpha(z_1) - \xi_p][\varepsilon^\beta(z_2) + \xi_p]} \\ &\quad + \frac{g^{\alpha\beta}(z_1, z_2) - 1}{[\varepsilon^\alpha(z_1) + \xi_p][\varepsilon^\beta(z_2) - \xi_p]}, \end{aligned} \quad (\text{A6})$$

where $g^{\alpha\beta}$ are the structure factors introduced in¹⁶ as

$$g^{\alpha\beta}(z_1, z_2) = \frac{\tilde{\omega}^\alpha(z_1)\tilde{\omega}^\beta(z_2) + \tilde{\Delta}^\alpha(z_1)\tilde{\Delta}^\beta(z_2)}{\varepsilon^\alpha(z_1)\varepsilon^\beta(z_2)}. \quad (\text{A7})$$

While integrating over ξ_p , we close the integration contour in the upper half plane and use representation (A6) along with the property $\text{Im } \varepsilon^R(z) > 0$, $\text{Im } \varepsilon^A(z) < 0$. For example, integration of the product of two retarded Green's functions from Eq. (A5) yields

$$\int d\xi_p \text{tr} [G_p^R(z) G_p^R(z + \omega)] = -2\pi i \frac{g^{RR}(z, z + \omega) - 1}{\varepsilon^R(z) + \varepsilon^R(z + \omega)}. \quad (\text{A8})$$

Gathering contributions from all terms and using the symmetry $\varepsilon^R(-z) = -\varepsilon^A(z)$, we have

$$\begin{aligned} Q(\omega) &= \frac{1}{2} \int_{\omega_\Delta}^{\infty} dz \left[\tanh \frac{z + \omega}{2T} B - \tanh \frac{z}{2T} A \right] \\ &\quad + \frac{1}{2} \int_{\omega_\Delta - \omega}^{\omega_\Delta} dz \tanh \frac{z + \omega}{2T} B, \end{aligned} \quad (\text{A9})$$

where

$$A = \frac{g^{RR}(z + \omega, z) - 1}{\varepsilon^R(z + \omega) + \varepsilon^R(z)} + \frac{g^{RA}(z + \omega, z) + 1}{\varepsilon^R(z + \omega) - \varepsilon^A(z)}, \quad (\text{A10})$$

$$B = -\frac{g^{AA}(z + \omega, z) - 1}{\varepsilon^A(z + \omega) + \varepsilon^A(z)} + \frac{g^{RA}(z + \omega, z) + 1}{\varepsilon^R(z + \omega) - \varepsilon^A(z)}. \quad (\text{A11})$$

We restrict ourselves to zero temperature. $B - A$ is real; thus, it does not contribute to the imaginary part of the response kernel and consequently to $\sigma'(\omega)$,

$$\sigma'(\omega) = \frac{ne^2}{m} \frac{Q''(\omega)}{\omega}. \quad (\text{A12})$$

The region of integration from $-\omega_\Delta$ to ω_Δ in the second integral in Eq. (A9) also gives a real contribution and can be omitted. Finally, neglecting the difference between ω_Δ and Δ that gives higher-order corrections in λ , finally we have for $Q''(\omega)$

$$Q''(\omega) = \frac{1}{2} \int_{\Delta - \omega}^{\Delta} dz \text{Im } B, \quad (\text{A13})$$

which coincides with Eq. (30) used in Sec. II B.

In order to calculate the conductivity we use the imaginary part of $\tilde{\omega}^{R,A}(z)$ and $\tilde{\Delta}^{R,A}(z)$, Eqs. (16) and (17). We work to leading order in the coupling constant; therefore, we expand B in Eq. (A13) and extract its imaginary part.

An imaginary contribution to B comes only from the imaginary corrections to the self-energy, $\tilde{\omega}^{R''}(z)$ and $\tilde{\Delta}^{R''}(z)$, Eqs. (21) and (22). They are proportional to the coupling

constant; thus, we expand in them. First, we expand $\varepsilon^{R,A}(z)$,

$$\varepsilon^{R,A}(z) = \varepsilon(z) \operatorname{sgn} z \pm i\Gamma^R(z), \quad (\text{A14})$$

with short-hand notation:

$$\varepsilon(z) = \sqrt{z^2 - \Delta^2}, \quad (\text{A15})$$

$$\Gamma^R(z) = \pi\omega_E\lambda \frac{\theta(|z| - \Delta - \omega_E)|z|(|z| - \omega_E) - \Delta^2}{2\sqrt{z^2 - \Delta^2}\sqrt{(|z| - \omega_E)^2 - \Delta^2}}. \quad (\text{A16})$$

Using the expansion of $\varepsilon^{R,A}(z)$ we expand the structure factors and numerators in (A11). After some calculation we get

$$\begin{aligned} \frac{1}{2} \operatorname{Im} B = & -\frac{\Delta}{\omega\varepsilon(z)\varepsilon(z+\omega)} \left[\frac{\Delta\tilde{\omega}^{R''}(z) + z\tilde{\Delta}^{R''}(z)}{\varepsilon(z)} + \frac{\Delta\tilde{\omega}^{R''}(z+\omega) + (z+\omega)\tilde{\Delta}^{R''}(z+\omega)}{\varepsilon(z+\omega)} \right] \\ & + \frac{z(z+\omega) - \Delta^2}{\omega^2\varepsilon(z)\varepsilon(z+\omega)} [\Gamma^R(z) + \Gamma^R(z+\omega)]. \end{aligned} \quad (\text{A17})$$

To simplify this further we use the explicit form of $\tilde{\omega}^{R''}(z)$, $\tilde{\Delta}^{R''}(z)$, and $\Gamma^R(z)$. Inserting $\operatorname{Im} B$ into Eqs. (A12) and (A13) and changing integration variables yields

$$\sigma'(\omega) = \frac{ne^2}{m} \frac{\pi\omega_E\lambda}{\omega^3} \int_{-\gamma+\Delta}^{\gamma-\Delta} dt \frac{-(t+\gamma)(t-\gamma) + \Delta^2}{\sqrt{(t+\gamma)^2 - \Delta^2}\sqrt{(t-\gamma)^2 - \Delta^2}}, \quad (\text{A18})$$

where $\gamma = (\omega - \omega_E)/2$. This integral can be expressed through elliptic functions, resulting in Eq. (33).

¹P. A. Lee, N. Nagaosa, and X.-G. Wen, *Rev. Mod. Phys.* **78**, 17 (2006).

²R. Khasanov, A. Shengelaya, K. Conder, E. Morenzoni, I. M. Savić, and H. Keller, *J. Phys. Condens. Matter* **15**, L17 (2003).

³R. Khasanov, D. G. Eshchenko, H. Luetkens, E. Morenzoni, T. Prokscha, A. Suter, N. Garifianov, M. Mali, J. Roos, K. Conder, and H. Keller, *Phys. Rev. Lett.* **92**, 057602 (2004).

⁴V. J. Emery and S. A. Kivelson, *Nature (London)* **374**, 434 (1995).

⁵W. L. McMillan, *Phys. Rev.* **167**, 331 (1968).

⁶H. Iwasawa, J. F. Douglas, K. Sato, T. Masui, Y. Yoshida, Z. Sun, H. Eisaki, H. Bando, A. Ino, M. Arita, K. Shimada, H. Namatame, M. Taniguchi, S. Tajima, S. Uchida, T. Saitoh, D. S. Dessau, and Y. Aiura, *Phys. Rev. Lett.* **101**, 157005 (2008).

⁷Authors of Ref. 6 suggest that this is so-called breathing mode with $\Omega \sim 69$ meV coupled to the electrons with coupling parameter $\lambda \sim 0.6$ that can be estimated from mass renormalization.

⁸We note that there is earlier works that ascribe the isotope effect to a change in hole density by appealing to the breakdown of the adiabatic approximation [V. Z. Kresin and S. A. Wolf, *Phys. Rev. B* **49**, 3652 (1994); A. Bill, V. Z. Kresin, and S. A. Wolf, *ibid.* **57**, 10814 (1998)]. We consider this scenario unlikely to be applicable to cuprates.

⁹R. A. Ferrell and R. E. Glover, *Phys. Rev.* **109**, 1398 (1958).

¹⁰A. B. Migdal, *Zh. Eksp. Teor. Fiz.* **34**, 1438 (1958) [*Sov. Phys. JETP* **7**, 996 (1958)].

¹¹A. A. Abrikosov, L. P. Gorkov, and E. Dzyaloshinsky, *Methods of the Quantum Theory of Fields in Statistical Physics* (Prentice Hall, Englewood Cliffs, NJ, 1963).

¹²G. M. Eliashberg, *Sov. Phys. JETP* **11**, 696 (1960) [*Zh. Eksp. Teor. Fiz.* **38**, 966 (1960)].

¹³G. M. Eliashberg, *Sov. Phys. JETP* **12**, 1000 (1961) [*Zh. Eksp. Teor. Fiz.* **39**(5), 1437 (1960)].

¹⁴D. J. Scalapino, in *Superconductivity*, edited by R. D. Parks (M. Dekker, New York, 1969), Vol. 2, p. 1412.

¹⁵Account for ξ_p in the numerator of Green's function in the leading order gives the correction to the chemical potential that is small by parameter Δ^2/ϵ_F^2 (see Ref. 15).

¹⁶S. B. Nam, *Phys. Rev.* **156**, 470 (1967).

¹⁷T. Holstein, *Ann. Phys. (NY)* **29**, 410 (1969).

¹⁸P. B. Allen, *Phys. Rev. B* **3**, 305 (1971).

¹⁹M. Capone, C. Castellani, and M. Grilli, *Condens. Matter Phys.* **2010**, 920860 (2010).

²⁰A. Vaezi, e-print [arXiv:1009.4721](https://arxiv.org/abs/1009.4721).

²¹D. di Castro, M. Angst, D. G. Eshchenko, R. Khasanov, J. Roos, I. M. Savić, A. Shengelaya, S. L. Bud'ko, P. C. Canfield, K. Conder, J. Karpinski, S. M. Kazakov, R. A. Ribeiro, and H. Keller, *Phys. Rev. B* **70**, 014519 (2004).